UMT PRESS

Journal of Sustainability Science and Management
Journal Homepage: https://jssm.umt.edu.my
eISSN: 2672-7226
DOI: http://doi.org/10.46754/jssm.2026.07.009

OPTIMISATION OF PHOTOCATALYTIC DISINFECTION PROCESS OF CERIUM OXIDE–ZINC OXIDE HETEROSTRUCTURED PHOTOCATALYST AGAINST PATHOGENIC *Vibrio parahaemolyticus*

SHARIFAH ZAHRATUL ASHIRAH SYED ABDULLAH[1], NAZAITULSHILA RASIT[1], FAZILAH ARIFFIN[2] AND WAN RAFIZAH WAN ABDULLAH[1]*

[1]*Faculty of Ocean Engineering Technology, Universiti Malaysia Terengganu, 21030 Kuala Nerus, Terengganu, Malaysia*
[2]*Faculty of Science and Marine Environment, Universiti Malaysia Terengganu, 21030 Kuala Nerus, Terengganu, Malaysia*

**Corresponding author: wanrafizah@umt.edu.my*

ARTICLE INFO

Article History:
Received: 10 September 2025
Revised: 5 December 2025
Accepted: 5 February 2026
Published: -

Keywords:
Sustainability, disinfection, photocatalyst, zinc oxide

ABSTRACT

Seawater contamination with pathogenic bacteria, such as *Vibrio parahaemolyticus* (*V. parahaemolyticus*), remains a serious environmental concern in aquaculture and coastal communities. Conventional water treatment methods often fail to achieve efficient microbial inactivation, largely because resilient bacteria persist. This study synthesised a cerium oxide–zinc oxide (CeO_2–ZnO) heterostructured catalyst and evaluated its efficacy in the photocatalytic disinfection of *V. parahaemolyticus* under UV light irradiation. A full-factorial design was employed to optimise the disinfection process. The effects of three key variables, including UV irradiation time (15 minutes to 60 minutes), photocatalyst dosage (0.5 g/L to 2.0 g/L), and initial pH (6 to 9), on photocatalytic disinfection efficiency (%) were investigated. Analysis of variance (ANOVA) revealed that all three factors and their interactions have significant effects on the photocatalytic disinfection efficiency of the CeO_2–ZnO heterostructured catalyst. The optimal conditions for achieving maximum bacterial disinfection against *V. parahaemolyticus* (99.9% reduction in CFU) were identified at a photocatalyst dosage of 0.5 g/L, UV irradiation for 60 minutes and an initial pH of 6. The findings proved the potential of CeO_2–ZnO heterostructured catalyst as an effective alternative for sustainable water disinfection, particularly in aquaculture water treatment applications. The use of statistical optimisation ensures process efficiency and scalability.

Introduction

Waterborne pathogens continue to pose serious public health and environmental challenges, particularly in coastal regions. *Vibrio parahaemolyticus* (*V. parahaemolyticus*), a Gram-negative bacterium naturally present in marine environments, is among the most concerning due to its pathogenic potential. In humans, infections can result in gastroenteritis, wound infections, and septicaemia (Drake *et al.*, 2007; Wang *et al.*, 2015; Ndraha *et al.*, 2022). Beyond human health risks, *V. parahaemolyticus* also threatens aquaculture sustainability, as outbreaks in shrimp farming have been associated with Acute Hepatopancreatic Necrosis Disease (AHPND), leading to mass mortalities and severe economic losses (Orozco-Ochoa *et al.*, 2023; Saputra *et al.*, 2023). The ability of this pathogen to resist conventional antibiotics and to adapt across diverse environmental conditions makes its control increasingly challenging.

To address this challenge, photocatalytic disinfection has emerged as a promising alternative that reduces reliance on antibiotics and chemical disinfectants, thereby offering a more sustainable strategy for safeguarding aquatic ecosystems and food security (Liu *et al.*, 2021; Saravanan *et al.*, 2021; Ding *et al.*, 2024). By minimising chemical residues and promoting the reuse of water resources in aquaculture and coastal communities, photocatalytic disinfection contributes to the sustainable management of natural resources.

Among photocatalytic materials, cerium oxide–zinc oxide (CeO_2–ZnO) heterostructured photocatalysts have gained considerable attention due to their superior performance compared to individual oxides (Hezam *et al.*, 2021; Apostolescu *et al.*, 2023; Li *et al.*, 2025). Coupling the semiconductors has been shown to enhance photocatalytic performance by prolonging charge-carrier lifetimes, improving interfacial charge transfer to adsorbed substrates and extending light absorption into the visible region (Sang *et al.*, 2014). Ai *et al.* (2023) reported that their CeO_2–ZnO nanoheterojunction photocatalyst exhibited significantly higher photocatalytic activity compared to pure ZnO and pure CeO_2. This improvement was attributed to more effective separation of photogenerated charge carriers at the CeO_2–ZnO interface, thereby reducing recombination and enhancing overall photocatalytic efficiency. Thus, CeO_2–ZnO photocatalysts represent a technically robust and environmentally sustainable material for advanced disinfection applications.

Despite their potential, the effectiveness of photocatalytic disinfection is influenced by several operational parameters, including UV irradiation time, photocatalyst dosage, and solution pH (Saravanan *et al.*, 2021; Ding *et al.*, 2024; Liu *et al.*, 2024). The interdependence of these variables complicates process optimisation, which is essential to ensure both efficiency and practicality in real-world applications. Therefore, a systematic and statistically guided optimisation approach is necessary to identify the most effective combinations of operating conditions.

In this study, a CeO_2–ZnO heterostructured photocatalyst was synthesised and evaluated for its ability to inactivate *V. parahaemolyticus* under UV light irradiation. A full-factorial design was employed to optimise the disinfection process systematically. The aim was not only to achieve high disinfection efficiency but also to provide insights into developing a sustainable and scalable pathogen-control strategy that supports aquaculture biosecurity and the responsible management of natural resources.

Materials and Methods

Raw Materials

Several essential chemicals were selected and extensively used throughout the study. These chemicals include zinc oxide (ZnO), cerium (III) nitrate [$Ce(NO_3)_3$], citric acid ($C_6H_8O_7$), and cerium oxide (CeO_2).

Nano-ZnO (particle size of less than 50 nm, purity of 99.9%) was obtained as a commercial-grade chemical supplied by Sigma-Aldrich. This compound served as the primary host metal oxide in both the preparation and control of the photocatalyst.

Cerium (III) nitrate hexahydrate [$Ce(NO_3)_3.6H_2O$] with 99.9% purity was also supplied by Sigma-Aldrich. This chemical was used as the precursor for synthesising CeO_2 in the heterostructured photocatalyst formulation. In addition, commercial-grade cerium (IV) oxide (CeO_2) powder with 99.9% trace-metal purity from Sigma-Aldrich was utilised as a control material.

Citric acid anhydrous ($C_6H_8O_7$) with a purity of 99% was likewise obtained from Sigma-Aldrich. This chemical functioned as the complexing agent in the citrate gelation technique.

Synthesis of CeO_2–ZnO Photocatalyst

A CeO_2–ZnO photocatalyst with a molar ratio of 1:100 was synthesised using the citrate gelation technique followed by calcination. Cerium (III) nitrate [$Ce(NO_3)_3$], nano-ZnO, and citric acid ($C_6H_8O_7$) were dissolved in deionised water and heated at 70°C to 80°C to form a gel. The gel was dried at 110°C for 19 hours in a convective oven and subsequently calcined at 1,200°C for 5 hours in a muffle furnace. The calcined product, referred to as the CeO_2–ZnO heterostructured photocatalyst, was ground to a particle size of less than 60 µm and characterised by X-ray diffraction (XRD, Rigaku Miniflex II Model PW1710) and field-emission scanning electron microscopy (FESEM, JEOL JSM 7600F).

Experimental Design

A full factorial design (2^3) with two replicates was employed to evaluate the effects of three operational parameters (UV irradiation time, catalyst dosage, and initial pH) on the photocatalytic disinfection of *V. parahaemolyticus*. The response variable was photocatalytic disinfection efficiency, R_B, expressed as the percentage reduction in viable bacterial counts. A total of 16 experimental runs were conducted to ensure statistical robustness. Factor levels and coded values are summarised in Table 1.

The photocatalytic disinfection efficiency was calculated using Equation (1).

$$R_B(\%) = \frac{Initial\ bacteria\ count\left(\frac{CFU}{ml}\right) - Final\ bacterial\ count\left(\frac{CFU}{ml}\right)}{Initial\ bacteria\ count\left(\frac{CFU}{ml}\right)} \times 100 \quad (1)$$

Experimental design and statistical analyses were performed using Minitab 16 software.

Bacterial Strain and Photocatalytic Disinfection Experiments

The *V. parahaemolyticus* type strain was obtained from the Institute of Tropical Aquaculture (AKUATROP), Universiti Malaysia Terengganu. The bacteria were cultured aerobically at 37°C for 12 hours in Zobell marine broth using aseptic techniques. A 5 mL aliquot of culture (~10^9 CFU/mL) was inoculated into 45 mL of autoclaved seawater within the reactor system. The suspension was exposed to UV light in the presence of a CeO_2–ZnO photocatalyst (0.5 g/L to 2.0 g/L) for up to 60 minutes. Constant aeration was maintained throughout the experiment to optimise dissolved oxygen levels, thereby enhancing the photogeneration of reactive oxygen species (ROS). The pH of the solution was adjusted to pH 6-9, and the temperature was maintained at 30°C. Bacterial inactivation was monitored by enumerating colony-forming units (CFU/mL) at defined time intervals during UV exposure.

Results and Discussions

Phase Analysis and Morphology of CeO_2–ZnO Heterostructured Photocatalyst

The surface morphology of the synthesised CeO_2–ZnO photocatalyst, compared with that of pure ZnO, is shown in Figure 1. The Scanning Electron Microscope (SEM) micrograph reveals clear phase segregation, with the CeO_2 phase (brighter due to its higher atomic number) preferentially distributed as nodular deposits on the ZnO grain surfaces.

Table 1: Experimental variables and levels

Factors (Independent Variables)	Levels	Actual Value	Coded Value	Response (Dependent Variable)
UV irradiation time, X_A	Low	15 minutes	-1	Photocatalytic disinfection efficiency, R_B (%)
	High	60 minutes	+1	
Catalyst dosage, X_B	Low	0.5 g/L	-1	
	High	2.0 g/L	+1	
Initial pH, X_C	Low	6	-1	
	High	9	+1	

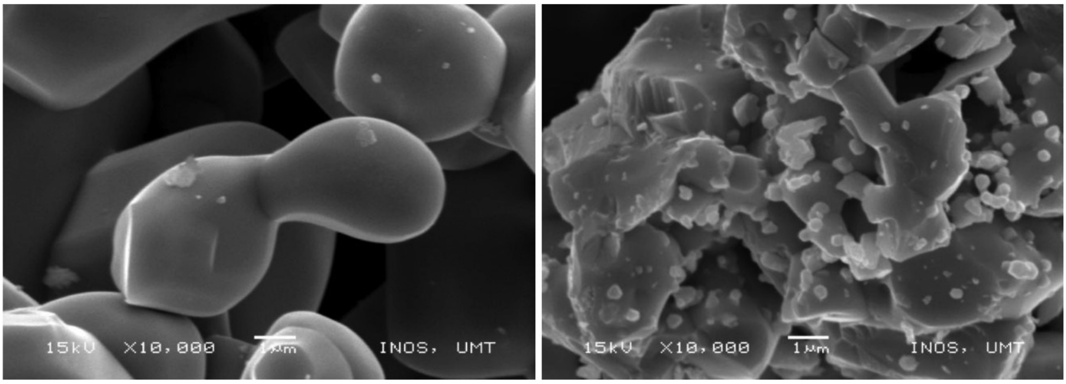

(a) (b)

Figure 1: SEM images of (a) calcined pure ZnO and (b) CeO_2–ZnO heterostructured photocatalyst with a molar ratio of 1:100

These nodules effectively "decorate" the ZnO grains, suggesting the successful formation of heterojunctions between the two oxides. Such heterostructure formation is consistent with previous reports on CeO_2–ZnO photocatalysts (Fereidooni *et al.*, 2022; Pathak *et al.*, 2024). The formation of heterojunctions is critical because it enhances charge separation and reduces electron-hole recombination, thereby improving photocatalytic activity.

The XRD patterns presented in Figure 2 further confirmed the coexistence of CeO_2 and ZnO phases within the heterostructured photocatalyst. The control ZnO sample exhibited diffraction peaks corresponding to the wurtzite hexagonal structure (PDF 80-75), while the CeO_2–ZnO samples displayed additional peaks characteristic of the cubic fluorite structure of CeO_2 (PDF 81-792). These results demonstrate that the citrate gelation and calcination approach successfully yielded a CeO_2–ZnO heterostructure with distinct crystalline phases of both oxides.

Full Factorial Design (FFD) Results

Table 2 presents the experimental results of the photocatalytic disinfection experiments using a full factorial design (FFD) for seawater

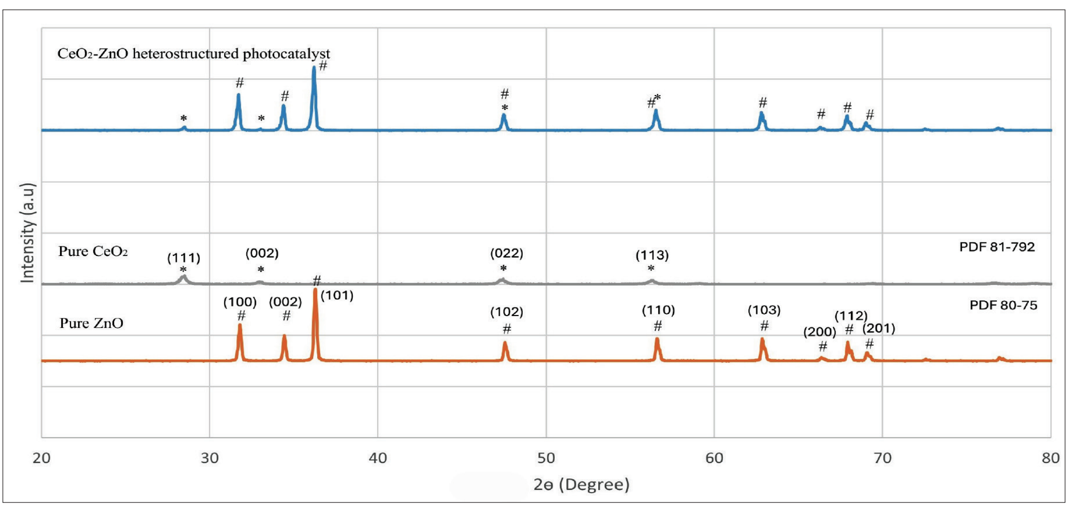

Figure 2: XRD patterns of (a) pure ZnO, (b) pure CeO_2, and (c) CeO_2–ZnO heterostructured photocatalyst

Table 2: FFD experimental data for photocatalytic disinfection efficiency, R_B of CeO_2–ZnO heterostructured photocatalyst against *V. parahaemolyticus*

Run. No.	Coded Value			Actual Value			Response
	X_A	X_B	X_C	UV Irradiation Time (minutes)	Catalyst Dosage (g/l)	Initial pH	Photocatalytic Disinfection Efficiency, R_B (%)
1	-1	-1	+1	15	0.5	9	98.00
2	-1	-1	+1	15	0.5	9	98.00
3	+1	-1	-1	60	0.5	6	99.90
4	+1	-1	+1	60	0.5	9	98.17
5	+1	+1	+1	60	2.0	9	99.50
6	+1	+1	-1	60	2.0	6	99.80
7	-1	+1	-1	15	2.0	6	97.70
8	+1	+1	-1	60	2.0	6	99.80
9	-1	+1	+1	15	2.0	9	94.00
10	+1	+1	+1	60	2.0	9	99.40
11	+1	-1	+1	60	0.5	9	98.40
12	-1	+1	-1	15	2.0	6	97.90
13	-1	+1	+1	5	2.0	9	95.00
14	-1	-1	-1	15	0.5	6	99.80
15	+1	-1	-1	60	0.5	6	99.90
16	-1	-1	-1	15	0.5	6	99.70

contaminated with *V. parahaemolyticus*. Within the studied parameter ranges of UV irradiation time, catalyst dosage, and initial pH, the CeO_2–ZnO heterostructured photocatalyst consistently achieved more than 95% disinfection efficiency under UV irradiation.

Similar to other semiconductor-based photocatalysts, the disinfection activity of CeO_2–ZnO is primarily light-driven. Upon UV illumination, the photocatalyst surface promotes electron-hole separation, initiating redox reactions that generate reactive oxygen species (ROS). These ROS such as hydroxyl radicals ($\cdot OH$) and superoxide anions ($\cdot O_2^-$) are highly reactive and cause irreversible microbial damage. The mechanisms of inactivation include lipid peroxidation of cell membranes (Dalrymple *et al.*, 2010), oxidation of proteins and enzymes (Zhao *et al.*, 2023), and nucleic acid degradation (Ge *et al.*, 2023), ultimately leading to cell wall rupture and bacterial death (Saravanan *et al.*, 2021). Importantly, this mechanism provided a sustainable alternative to conventional chemical disinfectants, minimising harmful chemical residues in water treatment and supporting safer, environmentally friendly disinfection practices.

The analysis of variance (ANOVA) summarised in Table 3 revealed that all studied factors, including UV irradiation time, catalyst dosage, and initial pH, as well as their interactions (UV irradiation time-pH, UV irradiation time-catalyst dosage), significantly influenced the disinfection efficiency of the CeO_2–ZnO photocatalyst. Significance was evaluated at the 95% confidence level, with p-values < 0.05 indicating a statistically meaningful effect. Table 4 lists all the coded coefficients for the model equation.

Table 3: ANOVA for photocatalytic disinfection efficiency, R_B of CeO_2–ZnO heterostructured photocatalyst against *V. parahaemolyticus*

Source	**DF**	**Adj. SS**	**Adj. MS**	**F-Value**	***p*-Value**
Model	7	46.0134	6.5733	93.66	0.000
Linear	3	30.9964	10.3321	147.22	0.000
UV irradiation time, X_A	1	13.8198	13.8198	196.92	0.000
Catalyst dosage, X_B	1	4.6981	4.6981	66.94	0.000
Initial pH, X_C	1	12.4786	12.4786	177.80	0.000
2-way Interactions	3	13.1057	4.3686	62.25	0.000
Catalyst Dosage*pH (X_BX_C)	1	0.0281	0.0281	0.40	0.545
UV irradiation time*pH (X_AX_C)	1	2.3028	2.3028	32.81	0.000
UV irradiation time*Catalyst Dosage (X_AX_B)	1	10.7748	10.7748	153.53	0.000
3-way Interactions	1	1.9113	1.9113	27.23	0.001
UV Irradiation time*Catalyst Dosage*initial pH ($X_AX_BX_C$)	1	1.9113	1.9113	27.23	0.001
Error	8	0.5615	0.0702		
Total	**15**	**46.5748**			

Table 4: Coded coefficients for model equation

Term	**Effect**	**Coef.**	**SE Coef.**	**T-Value**	***p*-Value**
Constant		98.4419	0.0662	1486.38	0.000
UV irradiation time	1.8588	0.9294	0.0662	14.03	0.000
Catalyst dosage	-1.0838	-0.5419	0.0662	-8.18	0.000
Initial pH	-1.7663	-0.8831	0.0662	-13.33	0.000
UV irradiation time*Catalyst dosage	1.6412	0.8206	0.0662	5.73	0.000
UV irradiation time*Initial pH	0.7588	0.3794	0.0662	5.73	0.000
Catalyst dosage*Initial pH	-0.0837	-0.0419	0.0662	-0.63	0.545
UV irradiation time*Catalyst dosage*Initial pH	0.6913	0.3456	0.0662	5.22	0.001

Among the factors, UV irradiation time emerged as the most dominant variable, exerting a strong positive influence on disinfection efficiency. In contrast, both catalyst dosage and initial pH were found to be less significant and generally exhibited a negative effect. Excess photocatalyst loading likely increased light scattering and particle agglomeration, reducing active surface exposure, while higher pH conditions may have altered surface charge interactions between the photocatalyst and bacterial cells, thereby suppressing ROS activity. These findings underscore the importance of optimising irradiation duration rather than relying solely on increased photocatalyst dosage for achieving efficient microbial inactivation.

The relationship between disinfection efficiency, R_B and the studied variables is described by the regression model in Equation (2). The model yielded a high coefficient of determination (R^2 = 0.9879, adjusted R^2 = 0.9774), confirming an excellent fit and predictive reliability for the photocatalytic disinfection process.

$$R_B = 98.4419 + 0.9294X_A - 0.5419X_B - 0.8831X_C + 0.8206X_AX_B + 0.3794X_AX_C - 0.0419X_BX_C + 0.3456X_AX_BX_C \quad (2)$$

Effect of Process Parameters on Photocatalytic Disinfection Efficiency

The main-effect plot in Figure 3 shows the effects of UV irradiation time, catalyst dosage, and initial pH on photocatalytic disinfection efficiency. A clear trend is observed in which prolonged UV irradiation significantly enhanced bacterial inactivation. In contrast, increasing catalyst dosage and initial pH reduced disinfection efficiency. Figure 3 further shows that maximum performance was achieved at extended irradiation time, low catalyst dosage, and slightly acidic conditions.

The interaction effects between the studied factors are presented in Figure 4. A strong interaction is evident between UV irradiation time and catalyst dosage, indicated by crossing lines in the interaction plot. At a high catalyst dosage (2.0 g/L), the efficiency increased more sharply with increasing irradiation time. A weaker yet notable interaction was observed between UV irradiation time and initial pH, with basic pH (pH 9) conditions leading to a steeper increase in disinfection efficiency as UV irradiation time increased from 15 to 60 minutes. These interactions demonstrate that while UV irradiation time is the dominant factor, the combined influence of catalyst dosage and pH cannot be overlooked in optimising photocatalytic disinfection.

The contour plot in Figure 5 provides a visual representation of the optimal operating window. High disinfection efficiency (>99%) was achieved in the dark green region, corresponding to long UV irradiation time, low catalyst dosage, and slightly acidic conditions (pH 6). Based on Table 5, the optimised conditions for maximum bacterial inactivation of *V. parahaemolyticus* (99.9% reduction in CFU/mL) were determined to be UV irradiation for 60 minutes, a catalyst dosage of 0.5 g/L, and an initial pH of 6. Validation experiments confirmed excellent agreement between predicted and experimental values, supporting the robustness of the model.

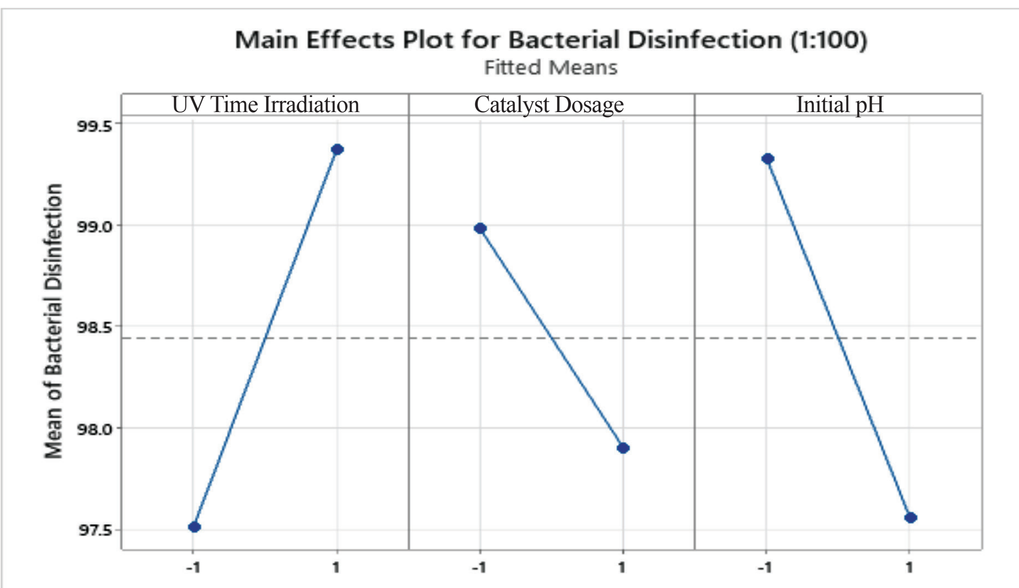

Figure 3: Individual effect of UV irradiation time, catalyst dosage, and initial pH on R_B of CeO_2–ZnO heterostructured photocatalyst

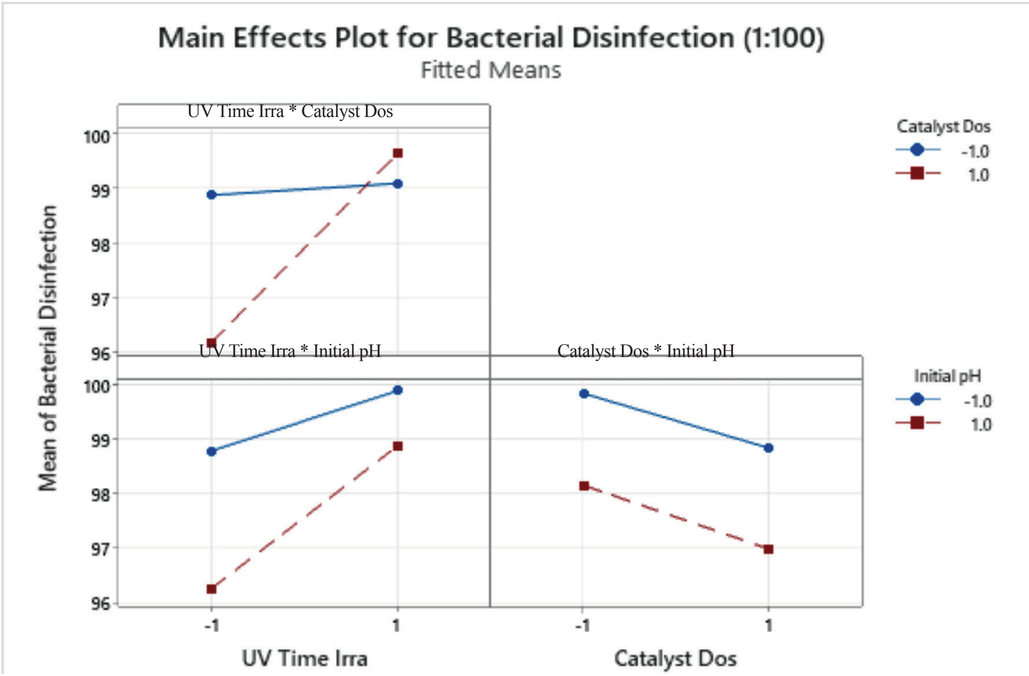

Figure 4: Interactive effect between UV irradiation time, catalyst dosage, and initial pH on R_B of CeO_2–ZnO heterostructured photocatalyst

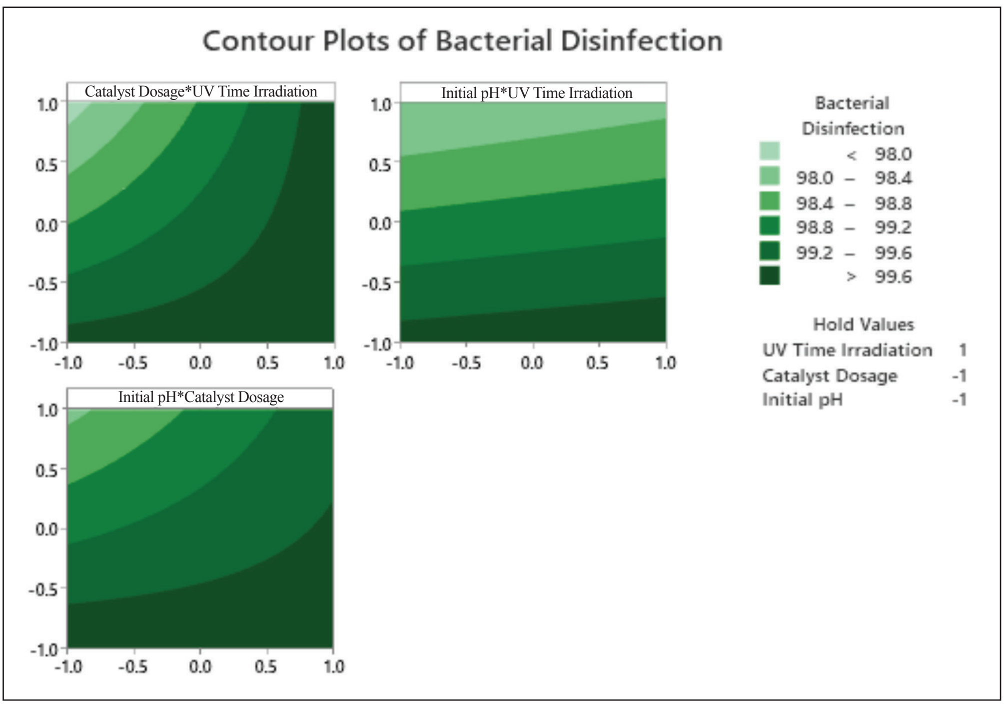

Figure 5: Contour plots for photocatalytic disinfection efficiency, R_B of CeO_2–ZnO heterostructured photocatalyst

Table 5: Optimisation solution for photocatalytic disinfection of *V. parahaemolyticus* using CeO_2–ZnO heterostructured photocatalyst under UV light irradiation

Sample	Optimisation Conditions	Optimisation Solution			R_B fit	Composite Desirability
		X_A	X_B	X_C		
CeO_2–ZnO with molar ratio of 1:100	Maximum R_B	+1	-1	-1	99.9	1

The photocatalytic disinfection effect was visually validated using agar plate assays (Figure 6). The untreated seawater (control) displayed dense *V. parahaemolyticus* growth (~10^9 CFU/mL), whereas the treated seawater showed near-complete bacterial elimination under optimised CeO_2–ZnO photocatalytic conditions. This strong bactericidal activity highlights the potential of the heterostructured catalyst to safeguard seawater quality.

Findings from this study indicate that photocatalytic disinfection using CeO_2–ZnO heterostructures was maximised under prolonged UV exposure, low catalyst dosage, and slightly acidic pH. Lower catalyst dosage provides sufficient active sites for ROS generation without inducing excessive light scattering or sedimentation, which can hinder photocatalytic activity (Jassby *et al.*, 2012). Prolonged irradiation ensures sustained ROS production, intensifying bacterial inactivation. Moreover, a slightly acidic pH enhances electrostatic attraction between the positively charged photocatalyst surface and the negatively charged bacterial cell membrane, thereby improving bacterial-photocatalyst contact and facilitating membrane rupture. These observations are consistent with previous findings on ZnO-based photocatalysts (Kazeminezhad & Sadollahkhani, 2016).

To the best of our knowledge, no prior study has reported the use of CeO_2–ZnO heterostructured photocatalysts for the inactivation of *V. parahaemolyticus* in seawater. This distinguishes the present work from existing literature, in which the antimicrobial performance of ZnO or CeO_2-based materials has been evaluated mainly against other bacterial strains and often without considering photocatalytic conditions. For instance, Sarwar *et al.* (2016) demonstrated that ZnO nanoparticles exhibit notable antimicrobial activity against *Vibrio cholerae* under non-photocatalytic conditions. More recently,

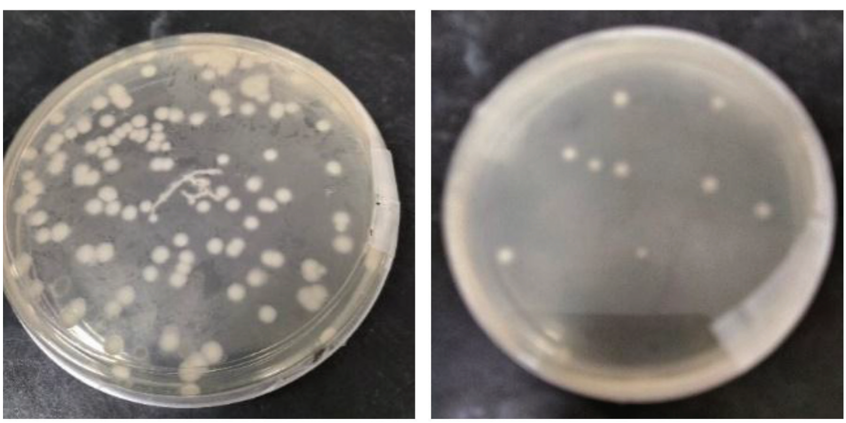

(a) (b)

Figure 6: The visual agar plate comparison of (a) untreated seawater and (b) treated seawater after exposure to 0.5 g/L of CeO_2–ZnO photocatalyst, 60 minutes of UV exposure, and pH 6

Jaafer *et al.* (2025) reported that their CeO_2–ZnO composites possessed inhibitory effects against *Staphylococcus aureus* and *Escherichia coli* using well-diffusion assays. However, these studies did not involve photocatalytic processes nor target *V. parahaemolyticus*. In contrast, CeO_2–ZnO synthesised in this work achieved nearly complete inactivation of *V. parahaemolyticus* in seawater under UV photocatalytic irradiation, highlighting the enhanced disinfection capability of the heterostructure and demonstrating its potential application in marine water treatment against

From a sustainability perspective, the optimised CeO_2–ZnO photocatalytic process demonstrates a promising, environmentally friendly alternative to conventional disinfection methods such as chlorination. Unlike chemical disinfectants that may generate harmful by-products, photocatalysis relies on light energy and reusable catalysts, reducing chemical consumption and residual contamination. Its ability to inactivate pathogenic bacteria in saline environments is particularly relevant for aquaculture, coastal water management, and safe seawater reuse, thus offering a green strategy to protect marine ecosystems and public health while reducing reliance on conventional chemical treatments.

Conclusions

This study demonstrated the effectiveness of a CeO_2–ZnO heterostructured photocatalyst for the disinfection of *V. parahaemolyticus* under UV light. A full factorial design revealed that UV irradiation time was the most significant factor, with catalyst dosage and pH also influencing disinfection performance through interactive effects. The optimal conditions for achieving 99.9% bacterial inactivation were identified at 60 minutes of UV exposure, 0.5 g/L catalyst dosage, and pH 6. These results highlight the potential of CeO_2–ZnO photocatalysts to deliver high disinfection efficiency under resource-efficient operating conditions. Importantly, the ability of this photocatalysis system to target pathogens in saline environments demonstrated strong potential for application in aquaculture biosecurity, coastal water quality management and safe water reuse.

Acknowledgements

The present study received financial support from the Talent and Publication Enhancement Research Grant (TAPE-RG) (Vot 55215), provided by Universiti Malaysia Terengganu and the Ministry of Higher Education, Malaysia.

Conflict of Interest Statement

The authors agree that this research was conducted in the absence of any self-benefit, commercial, or financial conflicts, and declare the absence of any conflicts of interest with the funders.

References

Ai, X., Yan, S., Lin, C., Lu, K., Chen, Y., & Ma, L. (2023). Facile fabrication of highly active CeO2@ZnO nanoheterojunction photocatalysts. *Nanomaterials*, *13*(8), 1371. https://doi.org/10.3390/nano13081371

Apostolescu, N., Tataru Farmus, R. E., Harja, M., Vizitiu, M. A., Cernatescu, C., Cobzaru, C., & Apostolescu, G. A. (2023). Photocatalytic removal of antibiotics from wastewater using the CeO_2/ZnO heterojunction. *Materials*, *16*(2), 850. https: //doi.org/10.3390/ma16020850

Dalrymple, O., Stefanakos, E., Trotz, M., & Goswami, D. (2010). A review of the mechanisms and modeling of photocatalytic disinfection. *Applied Catalysis B: Environmental*, *98*, 27–38. https://doi.org/10.1016/j.apcatb.2010.05.001

Ding, Y., Yang, G., Zheng, S., Gao, X., Xiang, Z., Gao, M., Wang, C., Liu, M., & Zhong, J. (2024). Advanced photocatalytic disinfection mechanisms and their challenges. *Journal of Environmental Management*, *366*, 121875. https://doi.org/10.1016/j.jenvman.2024.121875

Drake, S. L., DePaola, A., & Jaykus, L. A. (2007). An overview of *Vibrio vulnificus* and *Vibrio parahaemolyticus*. *Comprehensive Reviews in Food Science and Food Safety*, *6*(4), 120–144. https://doi.org/10.1111/j.1541-4337.2007.00022.x

Fereidooni, M., Esmaeilzadeh, F., & Zandifar, A. (2022). Innovatively synthesized CeO_2/ZnO photocatalysts by sono-photochemical deposition: Catalyst characterization and effect of operational parameters on high efficient dye removal. *Journal of Materials Science*, *57*(34), 16228–16244. https://doi.org/10.1007/s10853-022-07666-y

Ge, L., Wang, W., Tan, F., Wang, X., Qiao, X., & Wong, P. K. (2023). Advances in photocatalytic disinfection: Performances and mechanisms. *Solar RRL*, *7*(20), *2300446*. https://doi.org/10.1002/solr.202300446

Hezam, A., Wang, J., Drmosh, Q. A., Karthik, P., Bajiri, M. A., Namratha, K., Zare, M., Lakshmeesha, T. R., Shivanna, S., Cheng, C., & Byrappa, K. (2021). Rational construction of plasmonic Z-scheme Ag-ZnO-CeO_2 heterostructures for highly enhanced solar photocatalytic H2 evolution. *Applied Surface Science*, *541*, 148457. https://doi.org/10.1016/j.apsusc.2020.148457

Jaafer, M. D., Pasha, M. A., & Alkhayatt, A. H. O. (2025). Antimicrobial activity of ZnO-CeO_2 nanocomposites: Preparation, characterization, impact of Zn/Ce content. *Ceramics International*, *51*(5), 6533–6541. https://doi.org/10.1016/j.ceramint.2024.12.097

Jassby, D., Budarz, J. F., & Wiesner, M. (2012). Impact of aggregate size and structure on the photocatalytic properties of TiO_2 and ZnO nanoparticles. *Environmental Science & Technology*, *46*(13), 6934–6941. https://doi.org/10.1021/es202009h

Kazeminezhad, I., & Sadollahkhani, A. (2016). Influence of pH on the photocatalytic activity of ZnO nanoparticles. *Journal of Materials Science: Materials in Electronics*, *27*(5), 4206–4215. https://doi.org/10.1007/s10854-016-4284-0

Li, H., Wu, R., Ji, J., Liu, Y., Zhao, J., Sahar, S., & Zeb, A. (2025). Efficient CeO2/ZnO heterojunction for enhanced heterogeneous photocatalytic application. *Inorganic Chemistry Communications*, *171*, 113553. https://doi.org/10.1016/j.inoche.2024.113553

Liu, L., Shen, Z., & Wang, C. (2024). Recent advances and new insights on the construction of photocatalytic systems for environmental disinfection. *Journal of Environmental Management*, *353*, 120235. https://doi.org/10.1016/j.jenvman.2024.120235

Liu, N., Ming, J., Sharma, A., Sun, X., Kawazoe, N., Chen, G., & Yang, Y. (2021). Sustainable photocatalytic disinfection of four representative pathogenic bacteria isolated from real water environment by immobilized TiO_2-based composite and its mechanism. *Chemical Engineering Journal*, *426*, 131217. https://doi.org/10.1016/j.cej.2021.131217

Ndraha, N., Huang, L., Wu, V. C., & Hsiao, H. I. (2022). *Vibrio parahaemolyticus* in seafood: Recent progress in understanding influential factors at harvest and food-safety intervention approaches. *Current Opinion in Food Science*, *48*, 100927. https://doi.org/10.1016/j.cofs.2022.100927

Orozco-Ochoa, A. K., González-Gómez, J. P., Castro-del Campo, N., Lira-Morales, J. D., Martínez-Rodríguez, C. I., Gomez-Gil, B., & Chaidez, C. (2023). Characterization and genome analysis of six novel *Vibrio parahaemolyticus* phages associated with acute hepatopancreatic necrosis disease (AHPND). *Virus Research*, *323*, 198973. https://doi.org/10.1016/j.virusres.2022.198973

Pathak, V., Lad, P., Thakkar, A. B., Thakor, P., Deshpande, M. P., & Pandya, S. (2024). CeO_2-ZnO nano composites: Dualfunctionality for enhanced photocatalysis and biomedical applications. *Inorganic Chemistry Communications*, *159*, 111738. https://doi.org/10.1016/j.inoche.2023.111738

Sang, L., Zhao, Y., & Burda, C. (2014). TiO_2 nanoparticles as functional building blocks. *Chemical Reviews*, *114*(19), 9283–9318. https://doi.org/10.1021/cr400629p

Saputra, A., Maftuch, M., Andayani, S., & Yanuhar, U. (2023). Pathogenicity of *Vibrio parahaemolyticus* causing acute hepatopancreatic necrosis disease (AHPND) in shrimp (*Litopanaeus vannamei*) in Serang, Banten, Indonesia. *Biodiversitas Journal of Biological Diversity*, *24*(4), 2365–2373. https://doi.org/10.13057/biodiv/d240451

Saravanan, A., Kumar, P. S., Jeevanantham, S., Karishma, S., & Kiruthika, A. R. (2021). Photocatalytic disinfection of micro-organisms: Mechanisms and applications. *Environmental Technology & Innovation*, *24*, 101909. https://doi.org/10.1016/j.eti.2021.101909

Sarwar, S., Chakraborti, S., Bera, S., Sheikh, I. A., Hoque, K. M., & Chakrabarti, P. (2016). The antimicrobial activity of ZnO nanoparticles against *Vibrio cholerae*: Variation in response depends on biotype. *Nanomedicine: Nanotechnology, Biology and Medicine*, *12*(6), 1499–1509. https://doi.org/10.1016/j.nano.2016.02.006

Wang, R., Zhong, Y., Gu, X., Yuan, J., Saeed, A. F., & Wang, S. (2015). The pathogenesis, detection, and prevention of *Vibrio parahaemolyticus*. *Frontiers in Microbiology*, *6*, 144. https://doi.org/10.3389/fmicb.2015.00144

Zhao, D., Lu, H., Cheng, Q., Huang, Q., Ai, J., Zhang, Z., Liu, H., He, Z., & Li, Q. (2023). Research progress on inactivation of bacteriophages by visible-light photocatalytic composite materials: A mini review. *Materials*, *17*(1), 44. https://doi.org/10.3390/ma17010044